Food Chemistry: X 20 (2023) 101008

Contents lists available at ScienceDirect

Food Chemistry: X

journal homepage: www.sciencedirect.com/journal/food-chemistry-x

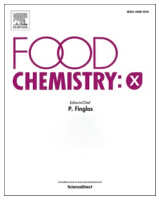

Exploring separation patterns and mechanisms of proanthocyanidins in grape seeds and pomace with diverse molecular weights, compositions, and structures

Xiaoyi Chen [a], Hong Song [a], Shubo Zhou [a], Chunlong Yuan [a,b,*], Junjun Li [a,*]

[a] College of Enology, Northwest A&F University, Yangling 712100, China
[b] Ningxia Helan Mountain's East Foothill Wine Experiment and Demonstration Station of Northwest A&F University, Yongning, Ningxia 750104, China

ARTICLE INFO

Keywords:
Proanthocyanidins
Adsorption kinetics
Reverse chromatography
Sephadex LH-20

Chemical compounds:
(+)-catechin (PubChem CID9064)
(−)-epicatechin (PubChem CID72276)
(−)-epicatechin gallate (PubChem CID107905)
(−)-epigallocatechin gallate (PubChem CID65064)
procyanidin B1 (PubChem CID11250133)
procyanidin B2 (PubChem CID122738)

ABSTRACT

The function of proanthocyanidins (PAs) relies on their structure and requires high-purity PAs. Though Sephadex LH-20 gel permeation chromatography (GPC) is expected to separate PAs based on structure, its usage rules and mechanisms remain unclear. This study delves into the PAs separation patterns on Sephadex LH-20, first confirming the purification mechanisms of PAs with various mean degrees of polymerization (DP) using the adsorption kinetic model. The study found that an increase in the molecular weight or mean DP of PAs results in decreased polarity, reduced hydrogen bonding actions, and intensified hydrophobic effect, causing delayed extraction of PAs on Sephadex LH-20, with galloylated PA as an exception, which was extracted first despite its high DP. Additionally, the principles for separating specific composition, such as monomers, dimers, etc., were evaluated. The study sheds light on enhancing the purification efficiency of PAs, thus advancing the precise separation technology of diverse proanthocyanidins.

Introduction

Proanthocyanidins (PAs), commonly known as condensed tannins, are characterized by flavan-3-ols with various patterns of hydroxylation patterns. The abundance of phenolic hydroxyl groups in PAs grants them natural antioxidant properties, which stabilize free radicals (Maulik, Das, & Dash, 1999). PAs, due to these biochemical attributes, have been associated with a range of therapeutic effects, such as anti-inflammatory (Diouf, Stevanovic, & Cloutier, 2009), anticancer (Unusan & Nurhan, 2020), antidiabetic (Tulini et al., 2016), and antidepressant activities (Jiang et al., 2017).

PAs are ubiquitously present in most plant-based foods. In wine, they primarily originate from grape skins and seeds, influencing various aspects of wine, including sensory characteristics, color stability, and the aging process (Chen et al., 2023; Wang et al., 2023b). However, only a small fraction of PAs is extracted during wine production (Rousserie, Rabot, & Geny-Denis, 2019), with the majority remaining in the grape pomace, thus, it is an excellent source for industrial PA production. Additionally, the biological effects of PAs depend on their composition and structural formation. Some researchers propose that the degree of polymerization (DP), which measures the number of recurring units in the polymer chain and specifies its molecular weight, significantly influences their properties (Yang et al., 2021). Studies indicate that PAs with different DP values exhibit varying therapeutic efficacy in various cell lines like oesophageal adenocarcinoma (OA) cells (Pierini et al., 2008), Caco-2 intestinal cells (Zumdick, Deters, & Hensel, 2012), and MCF-7 breast cancer cells (Li et al., 2015).

Due to the inherent complexity of PAs, which typically comprise a mixture of monomers, oligomers, and polymers, and their strong affinity for numerous adsorbents owing to the abundant hydroxyl groups, effective recovery becomes inherently challenging with conventional methods (Mottaghipisheh & Iriti, 2020; Rauf et al., 2019). Sephadex LH-20 gel permeation chromatography (GPC) is recognized as a classical technique for PA separation, characterized by its size-exclusion capacity and high-performance ion-exchange characteristics (Mottaghipisheh et al., 2020). Efficient PA separation, such as in applications involving *Rhus coriaria* L. (Kosar, Bozan, Temelli, & Baser, 2007), Japanese apricot (Horinishi et al., 2021), persimmon, and Loquat tree leaves (Tao et al.,

* Corresponding authors at: College of Enology, Northwest A&F University, No. 22, Xinong Road, Yangling, Shaanxi 710000, China.
E-mail addresses: yuanchl69@nwsuaf.edu.cn (C. Yuan), junjunli@nwafu.edu.cn (J. Li).

https://doi.org/10.1016/j.fochx.2023.101008
Received 16 October 2023; Received in revised form 13 November 2023; Accepted 13 November 2023
Available online 14 November 2023

2022), is achieved through the application of reversed-phase elution with Sephadex LH-20 GPC.

Using highly purified and well-defined active ingredients is a fundamental requirement in pharmacological research (Rauf et al., 2019). However, the complexity of PAs, with their wide range of molecular weights and intricate molecular structures, presents a challenge in precisely separating PAs with varying molecular weights or structural (Mottaghipisheh et al., 2020; Tian et al., 2018). Currently, Sephadex LH-20 GPC is one of the few techniques capable of separating and purifying milligram-to-gram quantities of PAs (Brown et al., 2017). In prior investigations, diverse researchers have explored various combination methods and elution procedures (e.g., mixtures of different solvents such as ethanol, methanol, and acetone) that can achieve PA separation based on the mean DP (Brown et al., 2017; Tao et al., 2022; Tibe, Meagher, Fraser, & Harding, 2011). However, few studies have yielded profound insights into the separation mechanisms and laws of PAs, and this led to the hindrance of the reasonable establishment of new separation schemes according to their requirements and made their research methodologies lack continuity and expansibility. Consequently, it is necessary to systematically investigate the separation regulations of PAs with different components and structures by Sephadex LH20 GPC and verify the separation mechanisms via adsorption kinetic models. Ultimately, by understanding the separation rules and mechanisms, one can independently and easily set up combination methods and elution procedures. Furthermore, there is a scarcity of reports on the extraction and fractionation of PAs from winemaking pomace, with most studies focusing solely on grape seeds. However, in practical production, the complete separation of seeds from pomace is a labor-intensive and inefficient process. Therefore, it is essential to elucidate the distinctions between these two raw materials.

Materials and methods

Materials and chemicals

Standards (purity >98 %) of (+)-catechin (C), (−)-epicatechin (EC), (+)-gallocatechin (GC), (−)-epicatechin gallate (ECG), (−)-epigallocatechin (EGC), (−)-epigallocatechin gallate (EGCG), procyanidin B1(PA-B1), and procyanidin B2(PA-B2) were purchased from Chromadex (Laguna Hills, CA, USA). HPLC-grade acetonitrile, methanol, and formic acid, along with analytical-grade vanillin, ascorbic acid, and concentrated hydrochloric acid, were obtained from XiLong Scientific (Guangdong, China). Phloroglucinol was purchased from Shyuanye (Shanghai, China). Sephadex LH-20 was obtained from General Electric Company (Boston, USA). Double-distilled water was used throughout the study.

Preparation of purificated PAs

The dried pomace, collected after fermentation from Pernod Ricard Wine Brewing Co., Ltd (Ningxia, China) in 2021, was sieved through a 5-mesh screen (particle diameter ≈ 4 mm) to remove larger impurities. Grape seeds were carefully isolated from a portion of the pomace. Subsequently, PAs were extracted and purified from grape pomace and seeds. Initially, both materials were crushed into fine powder and sifted through a 60-mesh sieve (particle diameter ≈ 0.25 mm). The powder underwent a 24-h *n*-hexane soak to remove oil. Afterwards, it was extracted with a 70 % ethanol solution for 12 h, with the extraction process repeated once. Finally, ethanol was evaporated, and the residue was freeze-dried to obtain crude PAs. Purification was accomplished using AB-8 macroporous resin, followed by freeze-drying to obtain purified PAs for subsequent fractionation based on mean DP (the purity of PAs after purification: seeds, 82.41±3.73 %; pomace, 79.81±1.99 %).

Fractionating PAs according to their mean DP

Program I: Separation tests were initially conducted using a small Sephadex LH-20 chromatography column (150×10 mm i.d.) to determine the extraction method. The activated Sephadex LH-20 gel was immersed in a 45 % (v/v) methanol aqueous solution for 12 h for stabilization. Subsequently, the gel was transferred slowly into the column. Purified PAs were dissolved in a 45 % (v/v) methanol aqueous solution at a concentration of 150 mg/mL and then applied to the column. Programs II and III followed the same packing column and sample loading methods. The column was successively rinsed with methanol aqueous solutions of 45 %, 55 %, 65 %, 75 %, 85 %, and 100 % (v/v), and any remaining substances were eluted with a 60 % (v/v) acetone aqueous solution. Each eluent had a total volume of 3 bed volumes (BV). To maintain consistent solvent transitions and prevent concentration effects during eluent changes, 1 BV of the recovered fraction was discarded before transitioning to the next eluent (the same as below). Records: the first fraction to the seventh fraction was labeled F1 – F7, where PF1 – PF7 represents the pomace fractions and SF1 – SF7 represents the seed fractions, the details in S1.

Program II: This program primarily illustrates the dynamic evolution of PA fractionation using the Sephadex LH-20 GPC technique. Purified PAs were loaded onto a small Sephadex LH-20 column (150×10 mm i.d.) and subsequently eluted with methanol aqueous solutions of 45 %, 75 %, and 100 % (v/v), followed by a 60 % (v/v) acetone aqueous solution. Fractions were collected at 1/2 BV intervals, with each eluant having a total volume of 3 BV. Six fractions were collected for each type of eluent, resulting in a total of 24 fractions for the entire process. Records: T1 – T4 for each group; T1-1 – T1-6 for each fraction of the T1 group; T2-1 – T2-6 for each fraction of the T2 group; T3-1 – T3-6 for each fraction of the T3 group; T4-1 – T4-6 for each fraction of T4 group; P for pomace fractions; S for seed fractions, the details in S1.

Program III: The effect of graded extraction was verified using different column sizes. Two types of glass columns were employed: a medium column (600×16 mm i.d.) and a large column (500×36 mm i.d.), resulting in resin beds of 400×16 mm i.d. and 400×36 mm i.d. The separation of purified grape seed PAs followed this optimized method: sequential elution with methanol aqueous water at concentrations of 45 %, 55 %, 65 %, 75 %, and 85 % (v/v), followed by elution with acetone aqueous water at 60 % (v/v), each time with an elution volume of 3 BV. The first 1 BV of the recovered fraction was discarded at the beginning. Records: M-F1 – M-F6 for each fraction from the medium column; L-F1 – L-F6 for each fraction from the large column, the details in S1.

All fractions were concentrated using a rotary evaporator and subsequently freeze-dried. The samples were stored in a −20 °C refrigerator for subsequent composition and structure determination.

Static and dynamic adsorption

Static adsorption

The static and dynamic adsorption method was employed based on a previously published procedure with slight modifications (Zhang, Sun, Duan, Chi, & Shi, 2023). Samples of PAs with varying mean DP were prepared using Program I and subsequently freeze-dried for future use. A 1.5 mg/ml sample solution was prepared with varying methanol content (0 %, 20 %, 40 %, 60 %, 80 %, 100 % (v/v)). Sephadex LH-20 gel (100 mg) was mixed with 5 mL of the sample solution and agitated at 120 rpm at 25 °C for 24 h. The adsorption extent (q, %) was calculated using the equation:

$$q = (C_0 - C_e)/C_0 \times 100\%$$

where C_0 and C_e are the concentrations of PAs before and after adsorption respectively (mg/L).

Dynamic adsorption

To investigate adsorption, 1 g of Sephadex LH-20 gel was added to

25 mL of sample solutions containing 2 mg/L of the target substance in 45 % methanol. Samples were taken at 5, 15, 30, 60, 120, and 240 min intervals for concentration determination. The adsorption quantity (qt, mg/g) was determined using the equation:

$$q = (C_0 - C_t)/m \times V$$

where C_0 is the sample concentration in the initial adsorption solution (mg/L); C_t is the sample concentration at time t; V is the volume of adsorption solution (mL); m is the mass of Sephadex LH-20 gel used for adsorption (g).

Adsorption kinetics

Pseudo-first-order (PFO) and pseudo-second-order (PSO) models were applied to analyze the factors influencing gel adsorption rates and to gain insights into the dynamics of the adsorption process (Yang, Wang, & Gu, 2023).

Pseudo-first-order equation: $\ln(q_e - q_t) = \ln q_e - k_1 t$

Pseudo-second-order equation: $t/q_t = 1/(k_2 q_e^2) + t/q_e$

where t is the adsorption time (min); q_e is the adsorption capacity per unit mass of adsorbent at equilibrium ($mg \cdot g^{-1}$); q_t is the adsorption capacity of the adsorbent at time t, ($mg \cdot g^{-1}$); k_1 (min^{-1}) and k_2 ($g \cdot (mg \cdot min)^{-1}$) are the rates constant of pseudo-first-order and pseudo-second-order, respectively.

PAs concentration

The concentration of PAs was determined using the vanillin assay as described previously (Gunaratne et al., 2013), with slight modifications. In brief, the sample (0.125 mL) was mixed sequentially with a 4 % (w/v) vanillin solution in methanol (0.75 mL) and hydrochloric acid (0.375 mL) in a tube. After thorough mixing, the mixture was incubated in a 30 °C water bath for 20 min, and the absorbance was measured. The control group was established by replacing the 4 % (w/v) vanillin solution with an equal volume of methanol while keeping all other conditions constant. Sample absorbance was measured at 500 nm using the Varioskan LUX automatic microplate reader (Thermo Fisher Scientific, Singapore). Sample concentration was calculated using the catechins standard curve ($Y = 0.7276 \times X + 0.0815$, $R^2 = 0.9996$), and results were expressed as mg catechin per Liter of the sample (mg catechin/mL).

Component analysis of PAs

HPLC analysis followed previously established methods (Wang, Yang, Zhang, & Yuan, 2022). An Agilent 1260 Infinity II series HPLC system (Agilent Technologies, Palo Alto, CA, USA) was employed for tannin analysis. The system comprised a degasser (G7122A), quaternary pump (G7111B), autosampler (G7129A), thermostated column compartment (G7116A), and diode array detector (G7115A). Separation was achieved using an ODS Hypersyl C18 LC column (125 mm × 4.6 mm, 5 μm, Thermo Scientific). The sample volume was 20 uL, with a flow rate of 0.80 mL/min, and a column temperature of 30 °C. Mobile-phase solvents included 1 % (v/v) formic acid in deionized water (A) and 1 % (v/v) formic acid in acetonitrile (B) with a gradient elution pattern: 0–10 min, 8 %; 10–20 min, 15 %; 20–40 min, 20 %; 40–45 min, 80 %; 45–50 min, 80 %; 51–56 min, 8 %. PAs peaks were detected at 280 nm. Monomer concentrations were determined using standard curves for C, EC, GC, ECG, EGC, EGCG, PA-B1, and PA-B2.

Structural analysis of PAs

Phloroglucinol was utilized for acid catalysis to determine the structure of PAs (Wang et al., 2022). Specifically, a solution of phloroglucinol reagent was prepared by dissolving 50 g of phloroglucinol and 10 g of ascorbic acid in 0.1 N HCl MeOH solution. Samples were mixed in a 1:1 (v/v) ratio with the phloroglucinol reagent and maintained at 50 °C for 20 min. The reaction was quenched by adding five times the volume of a 10 mM cold aqueous sodium acetate solution. The resulting samples were filtered through 0.45 μm polypropylene filters (Jinteng, Tianjin, China) into LC vials for HPLC analysis. For HPLC analysis, a reversed-phase chromatographic separation was performed using an ODS Hypersyl C18 LC column (125 mm × 4.6 mm, 5 μm, Thermo Scientific). The chromatographic conditions included a 20 μL sample volume, a flow rate of 0.60 mL/min, a column temperature of 30 °C, and mobile-phase solvents A (2 % formic acid in deionized water) and B (80:20 v/v acetonitrile/solvent A mixture). The gradient elution program was as follows: 0–5 min, 0 %; 5–35 min, 0–10 %; 35–65 min, 10–20 %. Subsequently, the column was washed and re-equilibrated. Chromatographic peaks were detected at 280 nm. The total moles of all subunits (flavan-3-ol monomer and phloroglucinol adducts) were determined. The total PA quantity, mean DP, and galloylation percentage (G%) were calculated following a previously established method (Des Gachons & Kennedy, 2003).

Statistical analysis

The two-way analysis of variance (ANOVA) assessed significant differences. GraphPad Prism 8 performed this analysis. Mean values ± standard deviations were calculated from three replicates per sample to represent the results. Origin 2021 (OriginLab Corporation, USA) conducted scatter plots, correlation analysis, and principal component analysis (PCA). Additionally, Origin 2021 handled fitting and plotting for the pseudo-first-order (PFO) and pseudo-second-order (PSO) models. The schematic diagram of the interaction were produced on Biorender's website and licensed for publication (https://www.biorender.com).

Results and discussion

Analysis of PAs separation fractions

Program I was employed to purify PAs from grape pomace and grape seeds into seven fractions labeled F1 to F7. Two HPLC methods determined their composition and structure. PA monomers and dimers were identified using standards, and PA structures were confirmed after depolymerization via acid catalysis with phloroglucinol (Jeffery, Mercurio, Herderich, Hayasaka, & Smith, 2008; Wang et al., 2022). In the composition chromatograms of fractions F1 to F7, the most prominent absorption peak occurred at 48.25 min (retention time, RT) (S2). This peak was particularly pronounced in samples F5 to F7, virtually constituting the only absorption peak. After depolymerization, typical PA subunits were observed in their structure (S2). Consequently, the peak in the composition chromatogram at 48.25 min (RT) was designated as one class of polymer PAs.

A total of six PA monomers and dimers were identified: C, EC, ECG, EGCG, PA-B1, and PA-B2; GC and EGC were not detected. Results indicated that the species and quantities of monomers and dimers gradually decreased during the elution process, and no single eluent completely extracted these substances (Fig. 1A). In F1, five monomers were detected, with ECG being the exception. It was speculated that the Sephadex LH-20 exhibits a strong retention effect on ECG, making it difficult to elute with lower concentration methanol solutions (≤45 %). C and EC have the highest content and longest elution times, while PA-B1 and PA-B2 elute more rapidly. All six monomers are present in F2, with F2 having the highest total monomer content (Fig. 1B). The primary difference in PA monomers between grape seeds and pomace lies in their concentration. In this study, grape pomace PA monomer content was notably higher. Research has shown that the amount of condensed tannins extractable from grape seeds can be up to 15 times that from grape skins, although concentration varies significantly by production area and year (Rousserie et al., 2019). For instance, in the Bordeaux region, the catechin content in grape seeds from Côtes de Bourg in 2007 was seven times that of Pauillac's grape seeds, with no significant

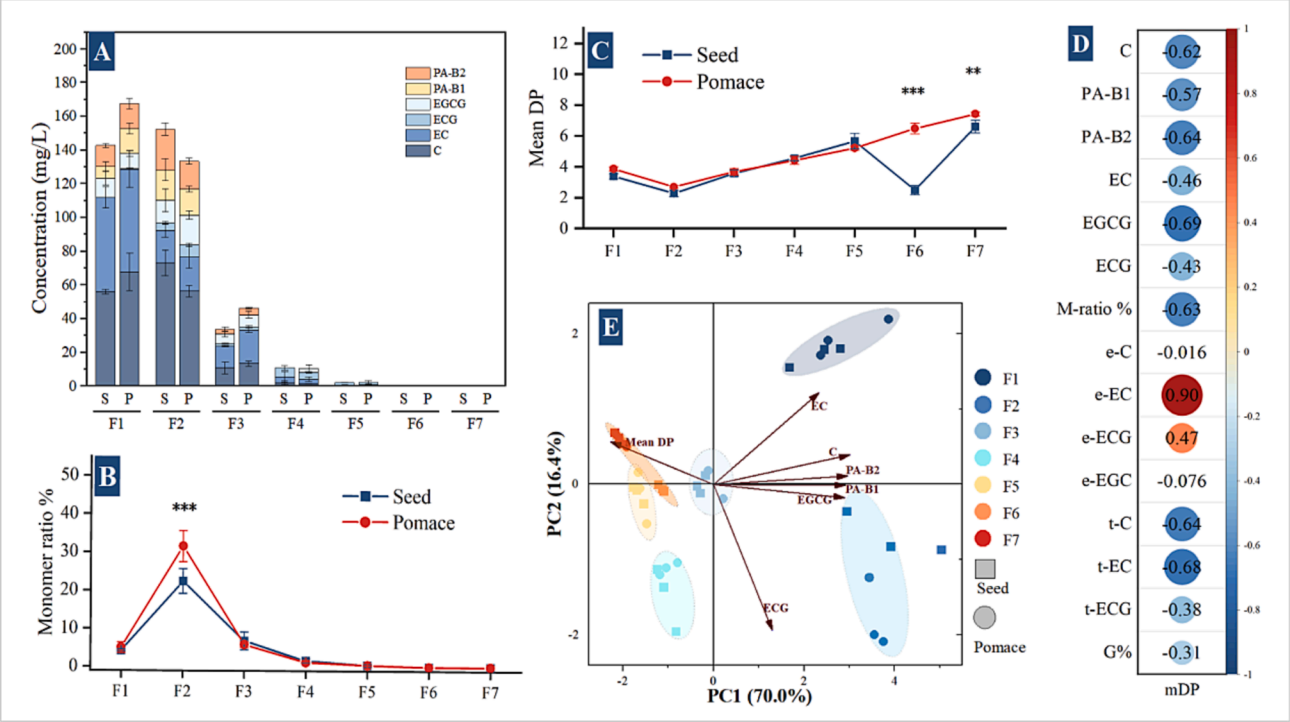

Fig. 1. Composition and structural analysis of different PAs fractions. (A) Composition and concentration of monomers (S for seed; P for pomace). (B) Comparative analysis of total monomer content ratio. (C) Comparative analysis of mean DP. (D) Correlation analysis of mean DP with monomers and subunits. (E) Principal component analysis based on composition and structure. $P < 0.05$, marked with *; $P < 0.01$, marked with **; $P < 0.001$, marked with ***.

difference observed in 2006 (Chira, Schmauch, Saucier, Fabre, & Teissedre, 2009).

A significant proportion of polymeric PAs is present in each fraction alongside PA monomers. The mean DP of F1 to F7 shows a gradual increase, but SF2, PF2, and SF6 exhibit smaller mean DPs (Fig. 1C). In a study involving the Sephadex LH-20 and Toyopearl HW-50F columns for the purification and fractionation of PAs from plant material, a consistent upward trend in the mean DP of the sample was observed (Brown et al., 2017). Correlation analysis revealed a strong negative correlation between the mean DP of samples and monomer content and total monomer proportion (Fig. 1D), resulting in SF2 and PF2 having the lowest mean DPs. Reversed-phase partition in reversed-phase solvents is performed by Sephadex LH-20 GPC, leading to the separation of substances with high polarity first. Typically, the fraction eluted first in reversed-phase elution has the lowest DP or molecular weight (Brown et al., 2017; Tao et al., 2022), indicating that F1 was initially expected to contain more monomers and the lowest mean DP. However, F1 exhibited a higher mean DP and a lower monomer ratio than F2. Further investigation is needed to understand the reasons behind this result.

Concerning PA structure, grape seed PAs consist of three types of extended subunits and three terminal subunits, while grape pomace PAs comprise four extended subunits and three types of terminal subunits (S3). The primary extended subunit is EC, and the main terminal subunit is C, consistent with previous reports (Tu et al., 2022; Zhang et al., 2017), with one study reporting that the main extended units of grape PAs being EC [accounting for 64.5 % (seeds) and 66.1 % (skin)] and the main terminal units being C [accounting for 42.5 % (seeds) and 57.5 % (skin)] (Rinaldi, Iturmendi, Jourdes, Teissedre, & Moio, 2015). A comprehensive PCA analysis was conducted to determine if Program I successfully separated these fractions based on their monomer content and mean DP (Fig. 1E). F1 and F2 share the same vector direction as the EC, C, PA-B2, PA-B1, ECG, and EGCG monomers, indicating significant influence by oligomers. Conversely, F6 and F7 align with the mean DP vector, suggesting a predominant influence by polymers. The PCA results demonstrate effective separation of F1 to F7, but components separated by equivalent eluents, such as SF1 and PF1, remain indistinguishable. This indicates that the method efficiently separates PAs based on molecular weight, with the choice of grape seeds or grape pomace as raw materials for purification having minimal impact on separation efficiency. The crude extracts of condensed tannins from the seven plant varieties were fractionated using varying concentrations of acetone aqueous solutions, as described by Brown et al. (2017). This process obtained 2–3 purified tannins with different mean degrees of polymerization were obtained. The researchers discovered that the plant varieties significantly influenced the mean DP and procyanidins/prodelphinidins (PC/PD) molar percentages in the condensed tannins. The DP and subunit composition of PAs significantly differed between the seeds and skins of fresh grapes. Previous studies have shown that the DP of PAs in the Cabernet Sauvignon grape skins were five times greater than those in grape seeds, while the content was only one-fifteenth of that in grape seeds (Rousserie et al., 2019). Therefore, the extraction of a substantial amount of PA from grape skins during maceration and fermentation was the possible reason for the minimal structural difference observed between grape seeds and pomace in this study.

Dynamic evolution of PAs fractionation

In Program II, 24 sample tubes were collected from four gradient elutions, with the elution volume identical to that in Program I. The majority of monomers were eluted in Program II by the initial two solvents (Fig. 2A). EGCG was the first monomer to elute extensively (fraction T1-2); followed by C, EC, PA-B1, and PA-B2 (fractions T1-4 and T1-5), with ECG being the final elution (fraction T2-2). Notably, ECG was not detected in any of the six T1 samples, confirming that a 45 % (v/v) methanol solution could not extract this monomer from the gel. An additional peak for C and EC was observed in fraction T2-2, indicating stronger retention of these monomers by Sephadex LH-20 compared to solvent competition forces. Consequently, separating the remaining monomers remained challenging even with prolonged elution time for T1. The highest percentage of total PA monomers in grape seeds and

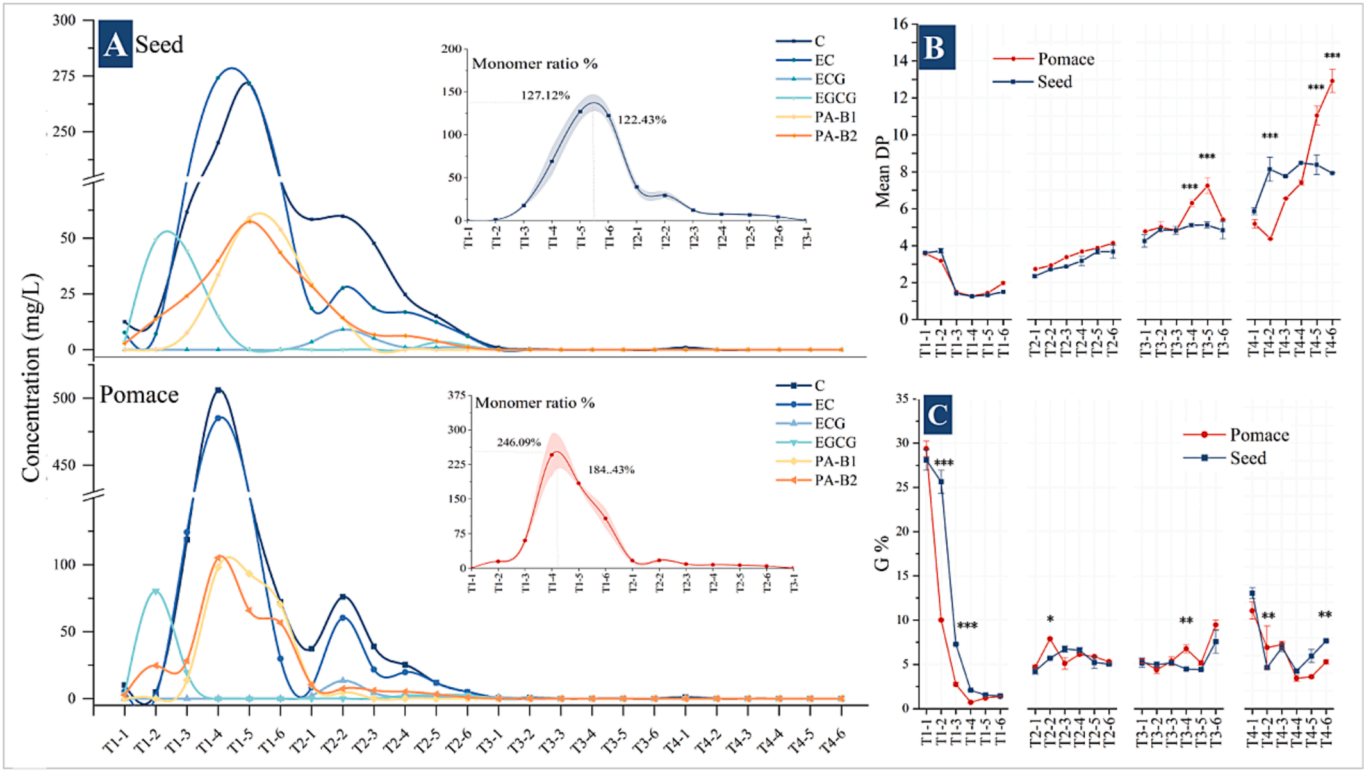

Fig. 2. Dynamic fractionation analysis. (A) Dynamic changes of monomers, and the total monomer ratio. (B) Dynamic changes of mean DP. (C) Dynamic changes of G%. $P < 0.05$, marked with *; $P < 0.01$, marked with **; $P < 0.001$, marked with ***.

pomaces was found in fractions PT1-4 and ST1-5, at 246.09 % and 127.12 %, respectively (Fig. 2A). While there are limited studies on Sephadex LH-20 separation of PA monomers, research on cocoa procyanidins extraction confirmed the gel's strong retention effect for C and EC, as they were detected in all four different fractions (Toro-Uribe, Herrero, Decker, López-Giraldo, & Ibáñez, 2020).

The mean DP of 24 fractions increased gradually, and the mean DP of the six sample tubes eluted with the same solvent also rose sequentially (Fig. 2B). Notably, T1-1 and T1-2 exhibited significantly higher mean DPs than other fractions in the same group, while T1-3 dramatically decreased to 1.41 (ST1-3) and 1.44 (PT1-3), respectively (S4). This phenomenon explains the higher mean DP of F1 compared to F2 in Program I. Sephadex LH-20 GPC incorporates both molecular sieving and reverse-phase partition effects. Interestingly, PAs in T1-1 and T1-2 exhibited an exceptionally high G% (Fig. 2C). PAs with a higher concentration of galloyl groups exhibit greater hydrophilicity (Wang, Dang, Zhu, & Li, 2021), intensifying solution competition over gel adsorption. The molecular sieving effect resulted in the faster elution of larger molecular weight substances that could not penetrate the gel's interior. Therefore, it is speculated that a combination of molecular sieving and distribution effects at the initial separation stage leads to preferential separation of highly hydrophilic galloylated PAs.

Furthermore, PT1-1 and PT1-2 did not detect the extended subunit EGC, characteristic of skin PAs (S4). Given that galloylated PAs are primarily found in grape seeds and are rare in the skin, it can be concluded that the separation primarily targets galloylated PAs in grape seed constituents during the initial stages. Galloylated PAs are crucial in the quality and nutritional functionality of wine. For instance, some studies suggest that a high proportion of galloylated PAs contributes to a "drying" taste in wine (Tu et al., 2022). In terms of biological activity, galloylated PAs strongly inhibited preadipocyte differentiation and the formation of lipid oxidation products compared to non-galloylated PAs (Zhu, Khalifa, Peng, & Li, 2017).

In Program II, the mean DP of samples eluted with 100 % methanol consistently differed from the results obtained in Program I. This discrepancy can be attributed to the limited elutability of residual PAs by methanol within the column, resulting from more extensive elution procedures in Program I. Considering that the results were not consistent, setting 100 % methanol elution in Program I appears unjustifiable. T4 samples were eluted using an acetone solution, with the mean DP of seed PAs stabilizing after reaching the maximum value. In contrast, the mean DP of pomace PAs continued to rise, reaching 12.91 (S2). The DP of PAs in grape skin significantly exceeded that in seeds (Chira et al., 2009), implying that raw materials exerted a more pronounced effect on high polymer PA fractionation and separation. Furthermore, correlation clustering was applied to the composition and structural data of all 24 sample tubes to confirm if the subdivided fractions still exhibited clustering based on all indicators (Fig. 3). The results indicate the consolidation of fractions into five categories: Class 1 comprises fractions containing PA monomers and low molecular weight PAs; Class 2 primarily comprising oligomeric PAs; Class 3 includes partial fractions of T1 and T4 characterized by a high G% in their PA structures. Additionally, most T4 and T3 fractions were classified as Class 4 and Class 5, respectively. Although this indicates that the subdivided fractions can be efficiently clustered according to their structural and compositional differences, unstable elution should be avoided when replacing the mobile phase. Most "unstable" fractions originated from T1-1, T2-1, and T4-1, possibly due to the eluent change. T1-1 and T1-2 had a high proportion of galloylated PAs, resulting in distinct structural and compositional differences as compared to other fractions in the same group. T4-1, obtained from the acetone aqueous phase instead of the methanol phase, possibly generated gel expansion volume variations and increased adsorption competition, thereby causing unstable separation of the fractions.

Adsorption kinetics

Static adsorption was performed on samples with different mean DP

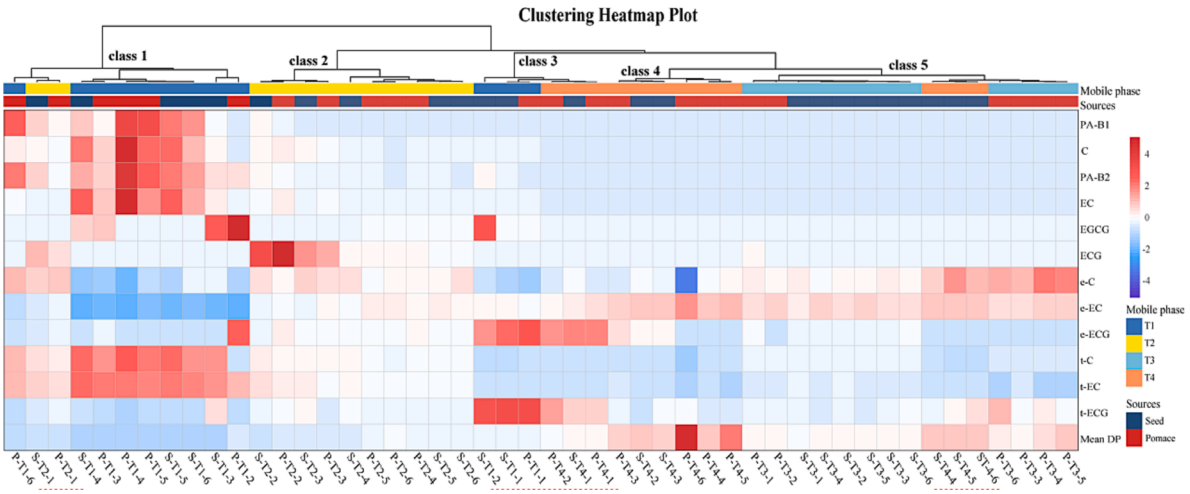

Fig. 3. Cluster analysis based on composition and structure for dynamic fractionation of PAs.

in methanol-aqueous solutions of varying concentrations to investigate the equilibrium adsorption capacity of Sephadex LH-20 GPC for PAs with different molecular weights or different mean DP (Fig. 4A). The role of methanol concentration in the adsorption process causes a significant difference in adsorption extents among various samples. Initially, samples F5 and F7 with high mean DP exhibited remarkably low adsorption in 0 % and 20 % (v/v) methanol-aqueous solutions. During the experiment, these samples showed poor solubility in water and low-concentration methanol solutions. This limited solubility likely contributed to their low adsorption extents. In low-concentration methanol-aqueous solutions, a similar insoluble condition was observed in the mixture of PAs extracted without fractionation (referred to as 'PAs' in Fig. 4). However, in a 40 % (v/v) methanol-aqueous solution, the adsorption extents rocketed to 90.35 % for F5 and 94.54 %

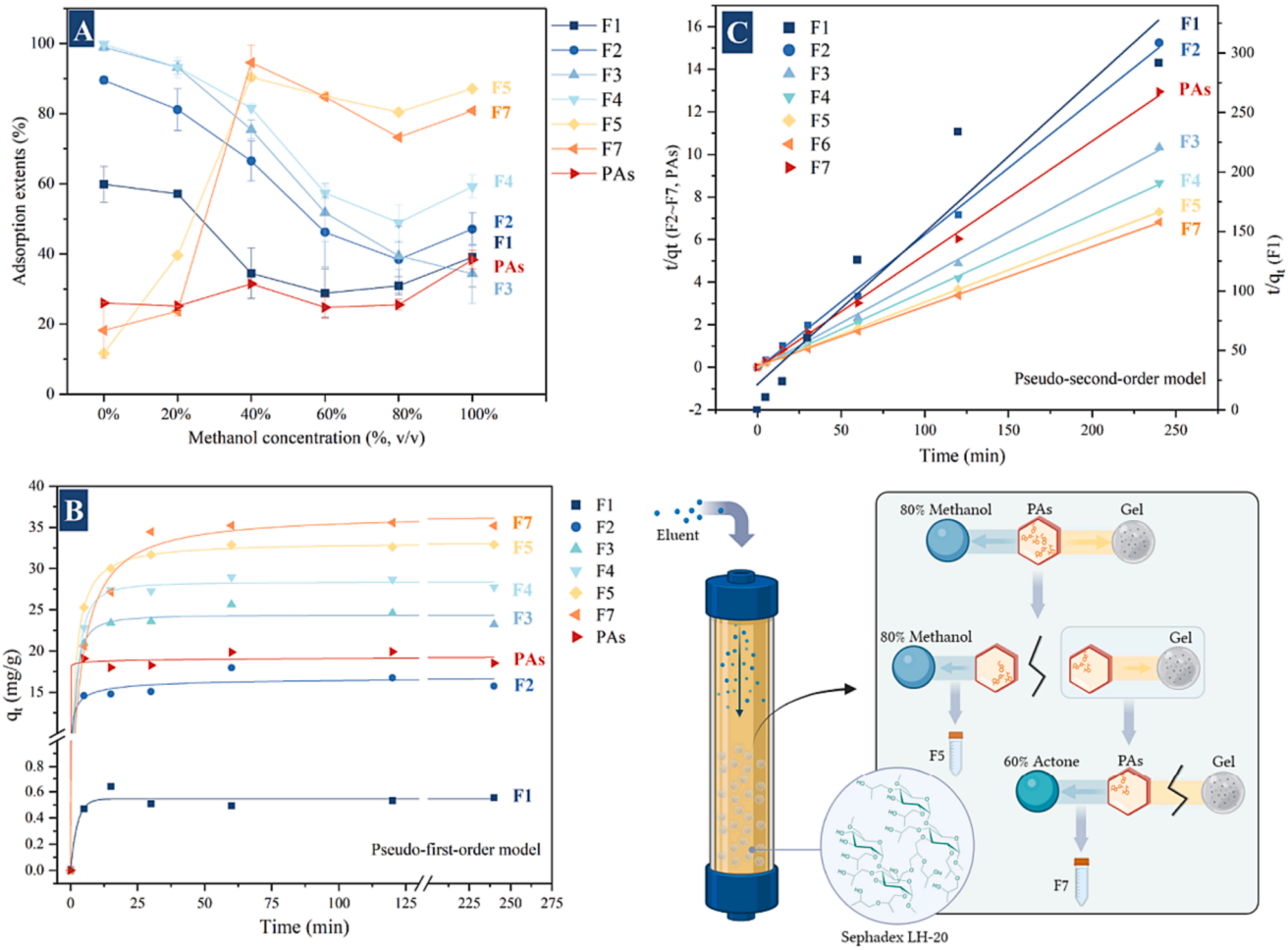

Fig. 4. Adsorption kinetics analysis of Sephadex LH-20 for PAs. (A) Static adsorption. (B) Pseudo-first-order kinetics plot. (C) Pseudo-second-order kinetics plot. (D) Schematic diagram of the interaction.

for F7, and maintained consistently high adsorption effectiveness to the end.

Furthermore, the adsorption extents of the gel for samples F1, F2, F3, and F4 in different methanol solution concentrations followed a consistent trend: as methanol concentration increased, adsorption extents decreased. This observation implies that increasing methanol concentration results in solvent competition that gradually supersedes the gel's adsorption effect. Fig. 4 illustrates that the gel's adsorption extent on samples in pure water (0 %) follows this sequence: F1 < F2 < F3 < F4, corresponding to an increase in their mean DP. As sample hydrophilicity increases, gel adsorption weakens, leading to a decrease in the adsorption rate in water (Soto, Moure, Domínguez, & Parajó, 2011). This observation suggests that PAs with lower mean DP exhibit higher hydrophilicity. Moreover, Sephadex LH-20 displayed a lower adsorption extent for the purified PAs mixture. Considering solubility and subsequent elution procedures, a starting concentration of 40 % (v/v) methanol-aqueous solution proved appropriate.

The PFO and the PSO fitting outcomes for different samples on the Sephadex LH-20 GPC are shown in Fig. 4B and C. The PFO model confirmed that Sephadex LH-20 gel had a fast adsorption rate for all samples within the initial 30 min. At 30 min, the adsorption for all samples, except F1, exceeded 95 % of the equilibrium adsorption amount, whereas F1 achieved only 59.60 % of the equilibrium adsorption. The adsorption amounts rank as follows: F7 > F5 > F4 > F3 > PAs > F2 > F1 (Fig. 4B). This study elucidated the direct correlation between the enhancement of the gel's adsorption effect and the increase in molecular weight of PAs in the case of complete sample dissolution. Additionally, the stronger retention of substances with lower polarity due to the reverse phase partition effect (Vailaya & Horvath, 1998) confirms that as molecular weight increases, the polarity of PA molecules decreases. The PSO model exhibits a higher correlation coefficient ($R_2^2 > R_1^2$), approaching 1 (Table 1). This suggests better fitting by PSO compared to PFO, and that the adsorption of PAs by Sephadex LH-20 is predominantly chemisorption. Furthermore, the calculated equilibrium adsorption amount ($q_{e,\ cal}$) closely aligns with the experimental equilibrium adsorption amount ($q_{e,\ exp}$), further validating the effectiveness of the PSO model in explaining the kinetic adsorption. While this result has not previously been reported for the separation of PAs, this research and analysis method has been widely employed in exploring the adsorption kinetics of chromatographic techniques (Wang et al., 2023a; Yang et al., 2023). The presence of hydroxyl and benzene groups in the structure of PAs suggests that hydrogen bonding and hydrophobic interactions are the primary driving forces for gel adsorption. Methanol acts as a competitive reagent for hydrophobic interaction, while water competes with hydrogen bonding reactions (Zhang et al., 2023). Using the example of the F5 and F7 samples with high mean DP, the gel's hydrophobic interaction competes with methanol, resulting in adsorbate desorption when methanol's competitiveness is strong (F5). Conversely, adsorption by the gel continues when methanol competition fails until desorption occurs with a stronger acetone solution (F7) (Fig. 4D).

Separation by different specifications of chromatography column

The comparative analysis of separation effects for different column sizes was necessary to replace small-size chromatographic columns when there is a high demand for extraction requirements. Two chromatographic column specifications were employed, resulting in six separate fractions (Table 2). Additionally, there were no significant differences in mean DP between corresponding samples from different chromatographic columns. Furthermore, M-F6 (23.47 %) and L-F6 (22.75 %) demonstrated the highest column recovery, characterized by a high mean DP, followed by M-F1 (16.22 %) and L-F1 (15.78 %), which had more monomers and oligomeric PAs. The medium-sized chromatography column yielded slightly higher recovery than the large-sized column, with a 7.21 % difference in total. The maximum total recovery reached 79.76 %, mainly attributed to the removal of 6 BV of transition eluent throughout the separation process. In one study, extracts fractionated from an acetone/water (7:1) solvent showed higher yields compared to other solvents, resulting in a total recovery of 93.54 % when separating PAs from mixed plant materials using Sephadex LH-20 GPC (Brown et al., 2017). Zhang et al. (2023) used Sephadex LH-20 GPC to separate EC, EGC, ECG, and EGCG standards with a 100 % elution rate. These findings suggest that column specifications only minimally impact the recovery of each fraction.

Conclusions

Based on their structures and constituents, the study separated proanthocyanidins by the Sephadex LH-20 gel permeation chromatography technique and revealed the dynamic fractionation laws and the adsorption kinetics mechanism. This confirmed the separation effectiveness of chromatography columns with different specifications. The study simultaneously analyzed the separation patterns of proanthocyanidin monomers (e.g., (+)-catechin, (−)-epicatechin, (−)-epicatechin gallate, (−)-epigallocatechin gallate, procyanidin B1, and procyanidin B2) extracted from plants. Adsorption kinetic experiments confirmed the dynamic fractionation hypothesis, thereby determining the adsorption and desorption kinetics for proanthocyanidins with varying degrees of polymerization, while elucidating the partial mechanism. However, subsequent research requires more advanced mass spectrometry to identify the composition and structure of each proanthocyanidin component. In summary, this study comprehensively analyzed and demonstrated the Sephadex LH-20 gel permeation chromatography fractionation mechanism for proanthocyanidins, thus establishing the foundation for future precision-based separation of proanthocyanidins with distinct structural details.

CRediT authorship contribution statement

Xiaoyi Chen: Conceptualization, Methodology, Formal analysis, Investigation, Writing – original draft, Writing – review & editing. **Hong Song:** Formal analysis, Methodology. **Shubo Zhou:** Resources, Writing – review & editing. **Chunlong Yuan:** Conceptualization, Funding

Table 1
Kinetics parameters for sample adsorption on Sephadex LH-20.

Sample	$q_{e,\ exp}$ (mg·g^{-1})	Pseudo-first-order model			Pseudo-second-order model		
		$q_{e,cal}$/(mg·g^{-1})	k_1/min^{-1}	R_1^2	$q_{e,cal}$/(mg·g^{-1})	k_2/[g·(mg·min)$^{-1}$]	R_2^2
F1	0.8545	0.6063	0.3063	0.7712	0.8140	0.0736	0.9172
F2	15.7490	16.0850	0.4697	0.9701	15.9084	0.0598	0.9981
F3	23.2395	24.1167	0.4043	0.9917	23.4082	0.0331	0.9988
F4	27.7342	28.0564	0.3340	0.9968	27.9096	0.1422	0.9996
F5	32.9123	32.1304	0.3014	0.9945	33.0251	0.0304	0.9999
F7	35.1873	34.7199	0.1466	0.9790	35.6125	0.0150	0.9995
PAs	18.5407	18.9274	0.4634	0.9894	18.7196	0.0533	0.9986

Note: exp, Equilibrium adsorption capacity determined from experiments; *cal,* Equilibrium adsorption amount calculated by fitting equation.

Table 2
Separation parameters for PAs sample by different specifications of column.

Column	Fraction	Monomer ratio %	Mean DP	G %	Purity %	Recovery %
Medium column (500×16 mm i.d.)	M-F1	100.54±7.29	1.47±0.07	1.48±0.24	81.02±6.52	16.22±1.08
	M-F2	30.76±4.21	2.77±0.14	5.87±0.49	96.86±3.73	11.34±1.28
	M-F3	5.25±0.39	3.89±0.12	10.13±1.27	109.89±1.86	10.06±0.75
	M-F4	0.63±0.06	4.78±0.17	9.86±0.91	112.69±0.93	11.55±1.46
	M-F5	0.14±0.02	5.59±0.27	11.74±2.06	110.83±8.38	7.12±1.06
	M-F6	0.02±0.02	7.45±0.40	10.55±0.97	115.48±1.86	23.47±1.15
Total						79.76±2.05
Large column (500×36 mm i.d.)	L-F1	112.73±9.66	1.40±0.13	1.30±0.54	83.82±3.19	15.78±1.32
	L-F2	29.46±5.62	2.79±0.32	3.43±1.11	87.01±3.19	12.77±0.86
	L-F3	8.30±0.62	3.81±0.38	6.66±0.81	103.77±2.00	9.79±0.57
	L-F4	1.65±0.14	4.90±0.56	8.15±1.23	114.95±3.99	8.70±1.11
	L-F5	0.25±0.01	5.90±0.43	7.28±0.78	106.57±3.59	5.09±0.74
	L-F6	0.00	8.03±0.17	9.16±0.12	117.34±0.80	22.75±2.39
Total						72.55±2.27

Note: Recovery%, calculated after freeze-drying by the equation: $R = m/M \times 100$ %, where m is the mass of the recovered fractions, and M is the mass of the loading sample onto the column; Purit%, calculated by the equation: $P = CV/M \times 100$ %, where C is the concentration of the sample, V is solution volume, and M is the mass of the sample.

acquisition, Supervision. **Junjun Li:** Funding acquisition, Supervision.

Declaration of Competing Interest

The authors declare that they have no known competing financial interests or personal relationships that could have appeared to influence the work reported in this paper.

Data availability

Data will be made available on request.

Funding

This work was supported by the Ningxia National Key Research and Development Program (no. 2021BEF02016).

Appendix A. Supplementary data

Supplementary data to this article can be found online at https://doi.org/10.1016/j.fochx.2023.101008.

References

Brown, R. H., Mueller-Harvey, I., Zeller, W. E., Reinhardt, L., Stringano, E., Gea, A., … Hardcastle, E. E. (2017). Facile purification of milligram to gram quantities of condensed tannins according to mean degree of polymerization and flavan-3-ol subunit composition. *Journal of Agricultural and Food Chemistry, 65*(36), 8072–8082. https://doi.org/10.1021/acs.jafc.7b03489

Chen, X., Liu, S., Yuan, J., Zhu, Y., Yuan, C., & Ren, Y. (2023). Application of different pre-fermentation techniques in the winemaking using Guankou table grape (*Vitis vinifera* × *Vitis labrusca*). *Food Bioscience, 51*, 1–13. https://doi.org/10.1016/j.fbio.2022.102272

Chira, K., Schmauch, G., Saucier, C., Fabre, S., & Teissedre, P. L. (2009). Grape variety effect on proanthocyanidin composition and sensory perception of skin and seed tannin extracts from bordeaux wine grapes (Cabernet Sauvignon and Merlot) for two consecutive vintages (2006 and 2007). *Journal of Agricultural and Food Chemistry, 57*, 545–553. https://doi.org/10.1021/jf802301g

Des Gachons, C. P., & Kennedy, J. A. (2003). Direct method for determining seed and skin proanthocyanidin extraction into red wine. *Journal of Agricultural and Food Chemistry, 51*, 5877–5881. https://doi.org/10.1021/jf034178r

Diouf, P. N., Stevanovic, T., & Cloutier, A. (2009). Study on chemical composition, antioxidant and anti-inflammatory activities of hot water extract from Picea mariana bark and its proanthocyanidin-rich fractions. *Food Chemistry, 113*(4), 897–902. https://doi.org/10.1016/j.foodchem.2008.08.016

Gunaratne, A., Wu, K., Li, D., Bentota, A., Corke, H., & Cai, Y.-Z. (2013). Antioxidant activity and nutritional quality of traditional red-grained rice varieties containing proanthocyanidins. *Food Chemistry, 138*(2–3), 1153–1161. https://doi.org/10.1016/j.foodchem.2012.11.129

Horinishi, A., Osaki, S., Masuda, T., Nomura, E., Tanaka, Y., Nakamura, Y.-I., … Ozaki, Y. (2021). Proanthocyanidin in the fruit of Japanese apricot (Prunus mume Sieb. et Zucc.) and their structural estimation by HPLC-ESI-MS/MS. *Journal of Food Composition and Analysis, 103*, Article 104039. https://doi.org/10.1016/j.jfca.2021.104039

Jeffery, D. W., Mercurio, M. D., Herderich, M. J., Hayasaka, Y., & Smith, P. A. (2008). Rapid isolation of red wine polymeric polyphenols by solid-phase extraction. *Journal of Agricultural and Food Chemistry, 56*, 2571–2580. https://doi.org/10.1021/jf073478w

Jiang, X., Liu, J., Lin, Q., Mao, K., Tian, F., Jing, C., … Pang, C. (2017). Proanthocyanidin prevents lipopolysaccharide-induced depressive-like behavior in mice via neuroinflammatory pathway. *Brain Research Bulletin, 135*, 40–46. https://doi.org/10.1016/j.brainresbull.2017.09.010

Kosar, M., Bozan, B., Temelli, F., & Baser, K. H. C. (2007). Antioxidant activity and phenolic composition of sumac (*Rhus coriaria L.*) extracts. *Food Chemistry, 103*(3), 952–959. https://doi.org/10.1016/j.foodchem.2006.09.049

Li, W., Liu, J., Guan, R., Chen, J., Yang, D., Zhao, Z., & Wang, D. (2015). Chemical characterization of procyanidins from Spatholobus suberectus and their antioxidative and anticancer activities. *Journal of Functional Foods, 12*, 468–477. https://doi.org/10.1016/j.jff.2014.11.009

Maulik, G., Das, D. K., & Dash, S. K. (1999). Oxygen free radical scavenging properties of proanthocyanidins. *Free Radical Biology and Medicine, 99*, 39.

Mottaghipisheh, J., & Iriti, M. (2020). Sephadex® LH-20, isolation, and purification of flavonoids from plant species: A comprehensive review. *Molecules, 25*(18), 4146. https://doi.org/10.3390/molecules25184146

Pierini, R., Kroon, P. A., Guyot, S., Ivory, K., Johnson, I. T., & Belshaw, N. J. (2008). Procyanidin effects on oesophageal adenocarcinoma cells strongly depend on flavan-3-ol degree of polymerization. *Molecular Nutrition & Food Research, 52*(12), 1399–1407. https://doi.org/10.1002/mnfr.200700513

Rauf, A., Imran, M., Abu-Izneid, T., Iahtisham Ul, H., Patel, S., Pan, X., … Rasul Suleria, H. A. (2019). Proanthocyanidins: A comprehensive review. *Biomedicine and Pharmacotherapy, 116*, Article 108999. https://doi.org/10.1016/j.biopha.2019.108999

Rinaldi, A., Iturmendi, N., Jourdes, M., Teissedre, P.-L., & Moio, L. (2015). Transfer of tannin characteristics from grape skins or seeds to wine-like solutions and their impact on potential astringency. *LWT - Food Science and Technology, 63*(1), 667–676. https://doi.org/10.1016/j.lwt.2015.02.037

Rousserie, P., Rabot, A., & Geny-Denis, L. (2019). From flavanols biosynthesis to wine tannins: What place for grape seeds? *Journal of Agricultural and Food Chemistry, 67*(5), 1325–1343. https://doi.org/10.1021/acs.jafc.8b05768

Soto, M. L., Moure, A., Domínguez, H., & Parajó, J. C. (2011). Recovery, concentration and purification of phenolic compounds by adsorption: A review. *Journal of Food Engineering, 105*(1), 1–27. https://doi.org/10.1016/j.jfoodeng.2011.02.010

Tao, W., Pan, H., Jiang, H., Wang, M., Ye, X., & Chen, S. (2022). Extraction and identification of proanthocyanidins from the leaves of persimmon and loquat. *Food Chemistry, 372*, Article 130780. https://doi.org/10.1016/j.foodchem.2021.130780

Tian, Y., Liimatainen, J., Puganen, A., Alakomi, H.-L., Sinkkonen, J., & Yang, B. (2018). Sephadex LH-20 fractionation and bioactivities of phenolic compounds from extracts of Finnish berry plants. *Food Research International, 113*, 115–130. https://doi.org/10.1016/j.foodres.2018.06.041

Tibe, O., Meagher, L. P., Fraser, K., & Harding, D. R. K. (2011). Condensed tannins and flavonoids from the Forage Legume Sulla (Hedysarum coronarium). *Journal of Agricultural and Food Chemistry, 59*(17), 9402–9409. https://doi.org/10.1021/jf2014759

Toro-Uribe, S., Herrero, M., Decker, E. A., López-Giraldo, L. J., & Ibáñez, E. (2020). Preparative separation of procyanidins from cocoa polyphenolic extract: Comparative study of different fractionation techniques. *Molecules, 25*(12), 2842. https://doi.org/10.3390/molecules25122842

Tu, Q., Liu, S., Li, Y., Zhang, L., Wang, Z., & Yuan, C. (2022). The effects of regions and the wine aging periods on the condensed tannin profiles and the astringency perceptions of Cabernet Sauvignon wines. *Food Chemistry: X, 15*, Article 100409. https://doi.org/10.1016/j.fochx.2022.100409

Tulini, F. L., Souza, V. B., Echalar-Barrientos, M. A., Thomazini, M., Pallone, E. M. J. A., & Favaro-Trindade, C. S. (2016). Development of solid lipid microparticles loaded with a proanthocyanidin-rich cinnamon extract (Cinnamomum zeylanicum): Potential for increasing antioxidant content in functional foods for diabetic population. *Food Research International, 85*, 10–18. https://doi.org/10.1016/j.foodres.2016.04.006

Unusan, & Nurhan. (2020). Proanthocyanidins in grape seeds: An updated review of their health benefits and potential uses in the food industry. *Journal of Functional Foods, 67*, Article 103861. https://doi.org/10.1016/j.jff.2020.103861

Vailaya, A., & Horvath, C. (1998). Retention in reversed-phase chromatography: Partition or adsorption? *Journal of Chromatography A, 829*, 1–27.

Wang, Z., Chen, X., Liu, Q., Zhang, L., Liu, S., Su, Y., … Yuan, C. (2023b). Untargeted metabolomics analysis based on LC-IM-QTOF-MS for discriminating geographical origin and vintage of Chinese red wine. *Food Research International, 165*, Article 112547. https://doi.org/10.1016/j.foodres.2023.112547

Wang, R., Dang, M., Zhu, W., & Li, C. (2021). Galloyl group in B-type proanthocyanidin dimers was responsible for its differential inhibitory activity on 3T3-L1 preadipocytes due to the strong lipid raft-perturbing potency. *Journal of Agricultural and Food Chemistry, 69*(17), 5216–5225. https://doi.org/10.1021/acs.jafc.1c00364

Wang, B., Wu, K., Liu, T., Cheng, Z., Liu, Y., Liu, Y., & Niu, Y. (2023a). Feasible synthesis of bifunctional polysilsesquioxane microspheres for robust adsorption of Hg(II) and Ag(I): Behavior and mechanism. *Journal of Hazardous Materials, 442*, Article 130121. https://doi.org/10.1016/j.jhazmat.2022.130121

Wang, Z., Yang, N., Zhang, J., & Yuan, C. (2022). Skin cell wall ripeness alters wine tannin profiles via modulating interaction with seed tannin during alcoholic fermentation. *Food Research International, 162*, Article 111974. https://doi.org/10.1016/j.foodres.2022.111974

Yang, H., Tuo, X., Wang, L., Tundis, R., Portillo, M. P., Simal-Gandara, J., … Deng, J. (2021). Bioactive procyanidins from dietary sources: The relationship between bioactivity and polymerization degree. *Trends in Food Science & Technology, 111*, 114–127. https://doi.org/10.1016/j.tifs.2021.02.063

Yang, T., Wang, N., & Gu, H. (2023). The adsorption behavior of niobium (V) on kaolin clay and kaolinite. *Applied Clay Science, 235*, Article 106866. https://doi.org/10.1016/j.clay.2023.106866

Zhang, S., Li, L., Cui, Y., Luo, L., Li, Y., Zhou, P., & Sun, B. (2017). Preparative high-speed counter-current chromatography separation of grape seed proanthocyanidins according to degree of polymerization. *Food Chemistry, 219*, 399–407. https://doi.org/10.1016/j.foodchem.2016.09.170

Zhang, Q., Sun, Q., Duan, X., Chi, Y., & Shi, B. (2023). Effectively recovering catechin compounds in the removal of caffeine from tea polyphenol extract by using hydrophobically modified collagen fiber. *Separation and Purification Technology, 322*, Article 124325. https://doi.org/10.1016/j.seppur.2023.124325

Zhu, W., Khalifa, I., Peng, J., & Li, C. (2017). Position and orientation of gallated proanthocyanidins in lipid bilayer membranes: Influence of polymerization degree and linkage type. *Journal of Biomolecular Structure and Dynamics, 36*(11), 2862–2875. https://doi.org/10.1080/07391102.2017.1369163

Zumdick, S., Deters, A., & Hensel, A. (2012). In vitro intestinal transport of oligomeric procyanidins (DP 2 to 4) across monolayers of Caco-2 cells. *Fitoterapia, 83*(7), 1210–1217. https://doi.org/10.1016/j.fitote.2012.06.013